This Supporting Information file was revised after publication. Please see the Addition and Correction (DOI: http://dx.doi.org/10.1021/jp900599h).

Supplementary information to the letter

Ionic liquid near a charged wall: structure and capacitance of electrical double layer, *M. V. Fedorov and A. A. Kornyshev*

1 Simulation Methodology

1.1 Model of ionic liquid

We consider a 1 to 1 mixture of counter-like singly charged spheres with a short-range repulsive Lennard-Jones potential $u_{LJ}^{ij}(r) = 2k_BT\left[\left(r_0^i + r_0^j\right)/r\right]^{12}$ between the particles i and j (k_B - Boltzmann constant, T - Temperature). The radii of the spheres r_0 were 0.5 nm for cations (r_0^c) and 0.25 nm for anions (r_0^a) reflecting typical asymmetry of ion sizes in ILs [1]. We screened all Coulomb interactions by an effective dielectric constant $\varepsilon^* = 2.0$, which accounts for electronic polarizability of the ions (see some discussion below). Masses of cations an anions were the same and were equal to 100 proton masses each.

1.2 Simulation cell

We put 1050 cations and 1050 anions between two electrodes in a rectangular unit box with periodic boundary condition in XY-direction. We took the box size in X and Y direction equal to 11 nm and 40 nm in Z direction. The electrodes were modeled as two parallel XY square lattices of densely packed Lennard-Jones spheres with r_0^w radii 0.11 nm; surface charge densities on the electrodes were varied by the partial charge of those spheres. No image forces were thus included into the simulation. To suppress the effects of periodicity of the simulation cell in Z-direction, each pair of electrodes was separated by the 24 nm distance filled by IL, and a 16 nm slab of vacuum separating each pair from the next periodic image in Z direction (see Figure S1). The inclusion of the vacuum slab into the unit cell was done to avoid artifacts from the periodic images in Z direction [2, 3].

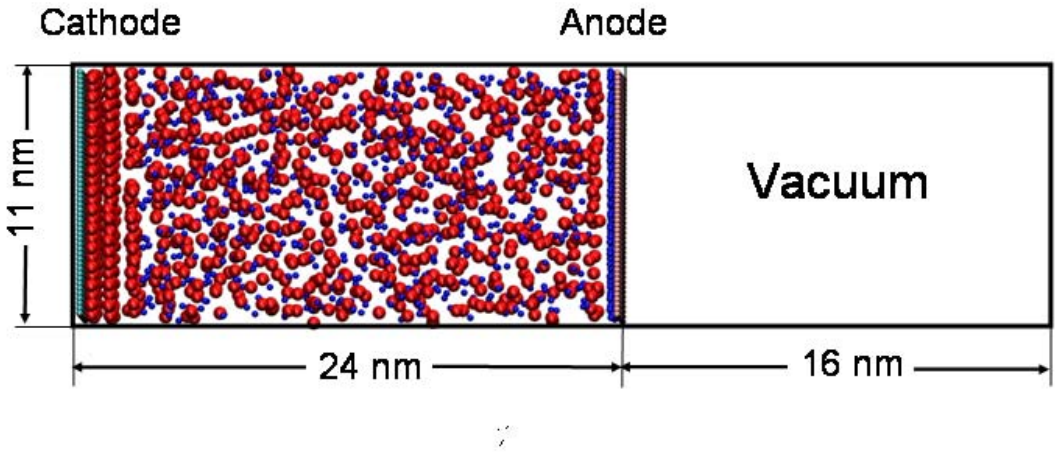

Figure S1. Geometry of the simulation cell shown in the XZ plane. Cations are shown as red spheres, anions are shown as blue spheres. The size of the particles is rescaled to make them more visible.

1.3 Algorithms

For molecular dynamics simulations we used Gromacs 3.3 software [4, 5]. The electrostatic interactions were treated with the use of Particle-Mesh Ewald summation with 3.0 nm real-space cut-off and some corrections for slab geometry proposed in [2, 3] which we briefly describe below. The Verlet algorithm has been used to integrate the equations of motion with a time step of 10 fs. We performed 24 molecular dynamic productive runs of 25 ns at constant box volume, number of particles and temperature, preceded by 10 ns equilibration runs. In all runs the simulation temperature was kept at 450 K using the Berendsen thermostat method [6]. Each run was performed for a given charge density of the electrodes σ in the interval between -80 to $+80$ μC/cm^2. We collected the data on the particle positions with 5 ps time interval.

1.4 Capacitance calculations

Using the obtained MD trajectories, for each value of σ we calculated the averaged charge distributions along the Z-axis $\rho(z)$ using a uniform grid with 0.025 nm distance between the nodes of the grid.

Then we calculated the total electrostatic potential Φ_t in the region between the electrodes as

$$\Phi_t(z) = \Phi_\sigma(z) + \Phi_{IL}(z), \qquad (1)$$

where Φ_σ is the potential of external electric field created by the charge on the electrodes, which is in the Gaussian system of units reads

$$\Phi_\sigma(z) = \frac{4\pi}{\varepsilon^*}\sigma z, \qquad (2)$$

Here ε^* is the effective dielectric constant of the `background medium' in which the ions are dissolved. Of course, there is no solvent and solutes in an ionic liquid -- there are only ions which form the `solvent' to themselves. Thus the introduction of a background dielectric constant screening Coulomb force-fields in the simulation is a trick, which is aimed to take into account the effects of electronic polarisability of the particles without explicitly considering it. Hence, then assuming $\varepsilon^* = 2$. Φ_{IL} is the potential of electric field

created by ions of the liquid in response to the external electric field, averaged over lateral *z*-crossection . This potential can be calculated using the solution of the Poisson equation as

$$\Phi_{IL}(z) = -\frac{4\pi}{\varepsilon^*}\int_0^z (z - z')\,\rho_{ion}(z')dz', \tag{3}$$

where $\rho_{ion}(z)$ is the charge density of ions averaged over lateral *z*-crossection. The integration was done numerically using the trapezoidal rule. Fig. S2. shows the potential profiles $U(z)$ across the simulation box in z - direction as

$$U(z) = \Phi_t(z) - \Phi_t(z_m), \tag{4}$$

where $z_m = 12$ nm which corresponds to the position of the middle of the IL slab. These curves reveal about 10 nm wide electroneutrality region in the middle of IL slab, so that the double layers at each electrode do not overlap. Hence we can consider each double layer separately.

Using these equations we obtain a relationship between the electrode surface charge density and the electrode potential, which is shown on Fig. S3. The numerical differentiation of this curve returns us the differential capacitance of one interface.

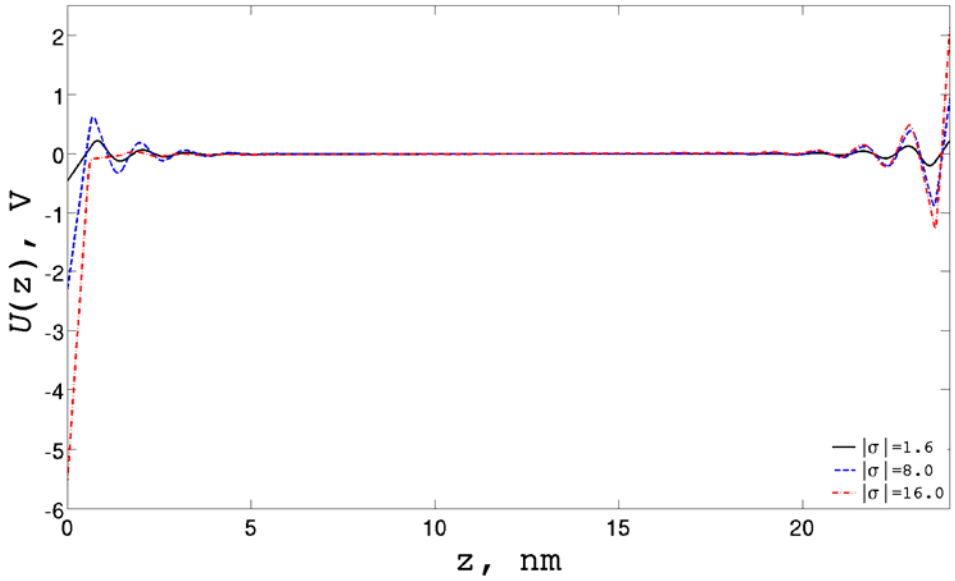

Figure S2. Potential profiles $U(z)$ across the simulation cell in Z direction. The potentials are shown for three different values of the absolute values of the charge density of the electrodes σ as labelled.

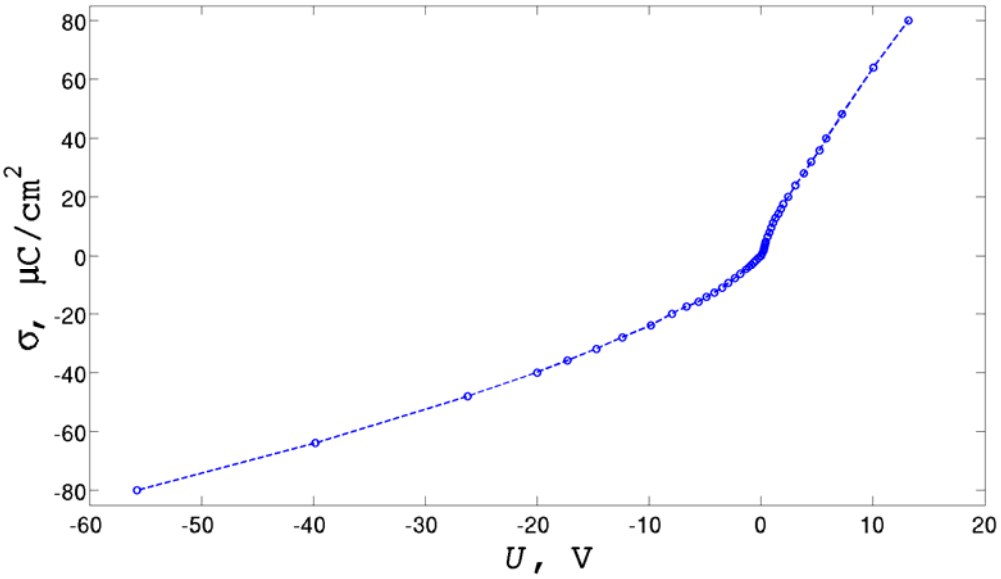

Figure S3. Relationship between the electrode surface charge density σ and the electrode potential *U***.** Points shown as circles are calculated from the results of molecular dynamic simulations performed for a model IL in which cations are twice as large as anions; to guide eye they are connected by dashed lines.

1.5 Potential of Zero Charge

We have estimated the potential drop between the electrode surface and the bulk of the gap in this model emerging spontaneously at zero charge of the electrode. To the accuracy of ± 1 mV we found this potential of about -23 mV $= 0.6\, k_b T$ at 450 K. This is indeed a small shift, but it is difficult to expect but it is difficult to expect the **p**otential of **z**ero **c**harge (pzc), U_0, to be substantially larger, as in the employed model we have neither specific adsorption, nor image forces. Still, just due to the entropy contribution, smaller anions statistically come closer to the electrodes than the cations, filling the voids between the latter. This minor excess of anions near the hard wall gives rise to this small negative spontaneous potential drop. Importantly, the position of the main maximum corresponds to $+300$ mV, relative to the bulk. Thus it is obvious that the *position of the maximum has nothing to do with the pzc*, unlike the situation of a mixture of ions of the same size [7]. There, at γ >1/3 (see the definition of γ below), the maximum should be at pzc, and pzc, measured relative to the bulk should be exactly equal to zero.

1.6 Correction to 3D Ewald summation for systems with slab geometry

Yeh and Berkowitz [2, 3] proposed an efficent way to calculate the electrostatic interactions for systems with slab geometry using the standard Ewald summation technique in conjunction to a correction term. Here, for the sake of completeness we briefly outline the main idea of the method, the details of which are well described in their papers [2, 3].

Let us consider a system of *N* point charges q_i with vector-coordinates r_i in a rectangular simulation cell with lengths $\{L_X, L_Y, L_Z\}$ in $\{X, Y, Z\}$ dimensions. Let as assume that the system satisfies the charge neutrality condition $\sum_{i=1}^{N} q_i = 0$.

When the boundary conditions are periodic in all three dimensions, there are few

standard algorithms of treating the electrostatic interactions in such systems using the 3D Ewald summation technique. One of the most popular is the Particle Mesh Ewald (PME) algorithm [8] which we are using in this work.

Generally, there exist some formulae for treating the electrostatic interactions in the case when only two dimensions (say, X and Y) are periodic - so called 2D Ewald summation technique [9]. However, this method is much more computationally expensive that the 3D-like method. One of the simplest approaches to employ the efficient 3D algorithms for a system with 2D geometry is to use a simulation cell with a slab of empty space in Z direction between the periodic images. For ion-molecular systems, it was done, e.g. in Ref. [10]. However, Spohr [11] and, later, Yeh and Berkowitz [2, 3] have shown, that, even with a slab which is four times larger than the maximal distance between the charges, this approach does not provide a reasonably accurate treatment of electrostatic interactions. Instead, Yeh and Berkowitz [2, 3] proposed an approximate correction term ΔF_i to the electrostatic force F_i acting on a particle with charge q_i, the $\{X,Y,Z\}$ components of which are given as

$$\begin{aligned} F_{X,i} &= F_{Y,i} = 0, \\ F_{Z,i} &= -\frac{4\pi q_i}{V} M_Z . \end{aligned} \tag{5}$$

where M_Z is the *z* component of the total dipole moment of the simulation cell M, and V is the volume of the unit simulation cell given by $L_X L_Y L_Z$. It has been shown in Ref. [2, 3], that this correction provides accurate treatment of electrostatic interactions when:

$$\Delta L_Z \geq L_X = L_Y , \tag{6}$$

where ΔL_Z is the thickness of the vacuum slab in the unit cell. We have used this technique in the present study, having set the geometry of our unit simulation cell to satisfy this condition.

2 Extended Mean-Field Theory

2.1 Diffuse layer capacitance

Modification of the mean-field theory of the diffuse double layer in ionic liquids, which takes into account the nonequal size of cations and anions was described in detail in Ref. [12]. In short, the equations that we have used in the main text of the Letter are Eq. (20) and Eq. (25) of Ref. [12].

$$C_d = C_0 \cosh\left(\frac{eU}{2k_B T}\right) \cdot \frac{1}{1+2\gamma \sinh^2\left(\frac{eU}{2k_B T}\right)} \cdot \sqrt{\frac{2\gamma \sinh^2\left(\frac{eU}{2k_B T}\right)}{\ln\left[1+2\gamma \sinh^2\left(\frac{eU}{2k_B T}\right)\right]}} \tag{7}$$

Here

$$C_0 = \frac{\varepsilon}{4\pi L_D} \tag{8}$$

is the linear Gouy-Chapman or ``Debye'' capacitance, in which $\frac{1}{L_D} \equiv \kappa = \sqrt{\frac{4\pi e^2 \overline{c}}{\varepsilon k_B T}}$ and $\overline{c}$ is the average salt concentration in the bulk, *e* is the elementary charge,

k_BT thermal energy, ε the intermediate frequency dielectric constant of ionic liquid, extrapolated from the height of a semicircle on a Bode impedance plot, the quantity close to 10 varying slightly from liquid to liquid [13]. [1]

Let us denote local concentrations of cations and anions as c^+ and c^- correspondingly. In the bulk $c^+ = c^- = c_0 = \overline{c}/2$. Let us introduce a parameter γ which reflects the sparsity of the particle packing in the liquid as [12]:

$$\gamma = \frac{2c_0}{c_{max}}, \tag{9}$$

where c_{max} is the maximal possible local concentration of ions (both cations as well as anions).

The dependence of γ on electrode potential will be approximated by a simple sigmoidal curve, interpolating between the value characteristic for the cation-rich layer and that of the-anion rich layer (positive electrode polarization):

$$\gamma(U) = \gamma_- + \frac{\gamma_+ - \gamma_-}{1 + \exp\left(e(U - U_0)/k_BT\right)}. \tag{10}$$

where $\gamma_+ \text{ and } \gamma_-$ are the γ parameters for cations and anions, correspondingly. When comparing the results of this approximation with our simulations, we determine the values of $\gamma_{+(-)}$ from the ratios of maximal cation (anion) density in the cation (anion) rich regions to the average ion density in the bulk. For our system we obtained $\gamma_+ = 0.5$, $\gamma_- = 0.07$. For simplicity we did not allocate any special voltage-scaling parameter that controls the rate of the transition between $\gamma_+ \text{ and } \gamma_-$ as a function of eU/k_BT .

2.2 Compact layer contribution.

To approximate the total capacitance we add a compact layer capacitance in series (Eq.(37) of Ref. [12]):

$$\frac{1}{C_{tot}} = \frac{1}{C_d} + \frac{1}{C_c} \tag{11}$$

Together with the expression for C_d this will comprise the **E**xtended **M**ean **F**ield **T**heory (EMFT).

Although the dependence of the compact layer contribution, C_c , could be quite complicated and include the properties of the metal (see the corresponding Section in Ref. [12], we assume here a simple Stern model, compatible with the level of `complexity' of our simulation model:

$$C_c = \tilde{\varepsilon}/4\pi d \tag{12}$$

Here *d* is the distance of the closest approach of an ion to the electrode surface, and $\tilde{\varepsilon}$ is the effective dielectric constant of the compact layer, the value somewhat smaller then ε. This is the only adjustable parameter of the Stern layer, because the dependence of *d* on electrode potential, in the spirit of our approximation for γ, is interpolated by the equation,

---

[1] This value of ε must not be confused with the value of ε^* , the electronic polarizability dielectric constant which screens the force-fields in our simulations. ε represents the dielectric response of all the ``dipole active degrees of freedom'' of the ionic liquid.

$$d(U) = r_- + \frac{r_+ - r_-}{1 + \exp\left(e(U - U_0)/k_B T\right)} \qquad (13)$$

where r_+, r_- are the Van der Waals radii of cations and anions, respectively.

2.3 Dielectric parameters

The values of dielectric constants used to plot the EMFT curve of Fig.1 for simplicity are taken the same as in Ref. [7] $\varepsilon = 7$, $\tilde{\varepsilon} = 5$. In principle, to compare the results with simulations, one should use the value of ε that corresponds to the simulated model. Such value could, in principle, be obtained via the MD simulations of the bulk dielectric properties [14] of a taken model of ionic liquid, reducing the number of adjustable parameters to one, $\tilde{\varepsilon}$. However, the accuracy of such calculations is usually low and in any case, we do not expect this value to be considerably different. The used values of ε and of $\tilde{\varepsilon}$ that provided good fit look very reasonable.

References

[1] Welton, T. *Chem. Rev.* **1999**, *99*, 2071.
[2] Yeh, I.; Berkowitz, M. *J. Chem. Phys.* **1999**, *111*, 3155.
[3] Yeh, I.; Berkowitz, M. *J. Chem. Phys.* **2000**, *112*, 10491.
[4] Berendsen, H. J. C.; van der Spoel, D.; van Drunen, R. *Comput. Phys. Commun.* **1995**, *91*, 43.
[5] Lindahl, E.; Hess, B.; van der Spoel, D. *J. Molec. Model.* **2001**, *7*, 306.
[6] Berendsen, H. J. C.; Postma, J. P. M.; van Gunsteren, W. F.; Dinola, A.; Haak, J. R. *J. Chem. Phys.* **1984**, *81*, 3684.
[7] Fedorov, M. V.; Kornyshev, A. A. *Electrochim. Acta* **2008**, *53*, 6835.
[8] Darden, T.; York, D.; Pedersen, L. *J. Chem. Phys.* **1993**, *98*, 10089.
[9] Heyes, D.; Barber, M.; Clarke, J. *J. Chem. Soc., Faraday Trans. II* **1977**, *73*, 1485.
[10] Pinilla, C.; Del Po'polo, M.; Kohanoff, J.; Lynden-Bell, R. *J. Phys. Chem. B* **2007**, *111*, 4877.
[11] Spohr, E. *J. Chem. Phys.* **1997**, *107*, 6342.
[12] Kornyshev, A. *J. Phys. Chem. B* **2007**, *111*, 5545.
[13] Daguenet, C.; Dyson, P.; Krossing, I.; Oleinikova, A.; Slattery, J.; Wakai, C.; Weingartner, H. *J. Phys. Chem. B* **2006**, *110*, 12682.
[14] Bopp, P. A.; Kornyshev, A. A.; Sutmann, G. *J. Chem. Phys.* **1998**, *109*, 1939.